Modelling the Diffusion Coefficients of Dilute Gaseous Solutes in Hydrocarbon Liquids

Yasser A. Aljeshi[1] · Malyanah Binti Mohd Taib[1] · J. P. Martin Trusler[1]

Abstract

In this work, we present a model, based on rough hard-sphere theory, for the tracer diffusion coefficients of gaseous solutes in non-polar liquids. This work extends an earlier model developed specifically for carbon dioxide in hydrocarbon liquids and establishes a general correlation for gaseous solutes in non-polar liquids. The solutes considered were light hydrocarbons, carbon dioxide, nitrogen and argon, while the solvents were all hydrocarbon liquids. Application of the model requires knowledge of the temperature-dependent molar core volumes of the solute and solvent, which can be determined from pure-component viscosity data, and a temperature-independent roughness factor which can be determined from a single diffusion coefficient measurement in the system of interest. The new model was found to correlate the experimental data with an average absolute relative deviation of 2.7 %. The model also successfully represents computer-simulation data for tracer diffusion coefficients of hard-sphere mixtures and reduces to the expected form for self-diffusion when the solute and solvent become identical.

1 Introduction

The diffusion coefficient is one of the key transport properties controlling many natural and industrial processes such as transport though membranes, interfacial mass transfer and pore-scale processes in hydrocarbon reservoirs. In recent years, the diffusion coefficients of light gases in hydrocarbon liquids have received significant attention, especially in connection with enhanced oil recovery (EOR) and geological carbon dioxide storage (GCS) [1, 2]. In EOR, natural gas, nitrogen or carbon dioxide

✉ J. P. Martin Trusler
   m.trusler@imperial.ac.uk

1   Department of Chemical Engineering, Imperial College London, South Kensington Campus, London SW7 2AZ, UK

is injected into an oil reservoir to maintain pressure, reduce oil viscosity and sweep the oil towards the production wells [3, 4]. In GCS, carbon dioxide is injected into, for example, a depleted hydrocarbon reservoir where it may dissolve into the reservoir fluids (brine and residual hydrocarbons). The rate of gas dissolution is controlled in part by diffusion and the diffusion coefficients are relevant parameters for modelling the process [5]. The diffusion coefficients for binary gas–liquid systems have been studied by means of experimental and computational methods. Due to the scarcity of experimental measurements under high-pressure conditions, correlations based on hydrodynamic and kinetic theories have been adopted to estimate the diffusion coefficients [6]. Several attempts have been made to develop a universal correlation based on kinetic theory but, to date, the available methods are restricted in scope. Therefore, the objective of the present work was to extend a kinetic theory-based model to cover a wide range of solutes (inorganic and light hydrocarbon gases) and solvents (the broad class of hydrocarbon liquids) at infinite dilution.

2 Existing Modelling Approaches

Numerous theoretical and empirical models have been developed for the estimation of binary diffusion coefficients for both the general case and for gas–liquid systems in particular. The two most common approaches incorporating elements of theory are the hydrodynamic approach and the methods based on the theory of rough hard-spheres. Both of these approaches are developed for the case in which one of the components is present at infinite dilution, corresponding to the so-called tracer diffusion coefficient.

2.1 Hydrodynamic Theory

The hydrodynamic theory is based on the Stokes–Einstein formula for the diffusivity of spherical particles in a continuum fluid and expresses the diffusion coefficient in terms of the thermal energy and the viscosity of the medium as follows:

$$D = \frac{k_B T}{n_{SE} \pi \eta a}. \tag{1}$$

Here, k_B is Boltzmann's constant, n_{SE} is the Stokes–Einstein number determined by the boundary condition at the surface of the spherical particles, η is the viscosity of the fluid and a is the radius of the spherical particles. For a no-slip boundary condition, $n_{SE} = 6$ [7] while, for a 'no-stick' boundary condition, $n_{SE} = 4$ [8]. When applied to non-spherical particles, a becomes the effective hydrodynamic radius.

Although based on hydrodynamic theory for macroscopic particles, the Stokes–Einstein equation is readily applied to molecular solutes in molecular solvents, usually with the assumption that $n_{SE} = 4$. The model then permits the diffusion coefficients of dilute solutes to be correlated with the viscosity of the solvent with a treated as an adjustable parameter. To obtain a good correlation, either a becomes temperature-dependent or the viscosity is raised to an empirical power [9].

This model is easily applied to correlate the diffusion coefficients of gaseous solutes in many different solvents as a function of temperature at constant pressure. When pressure is also a variable, matters are more complex and the observed behaviour is not captured well by making the hydrodynamic radius a function of temperature alone even when the pressure-dependence of the viscosity is included correctly. Cadogan et al. [10] and Taib et al. [11] found that a good correlation could be established in many cases by expressing the hydrodynamic radius as a function of the solvent density. However, such an approach was found to breakdown for highly viscous solvents such as squalane [10].

2.2 Kinetic Theory

The kinetic theory of dilute gases was extended to dense pure fluids by Enskog under the assumption of hard spherical molecules [8]. Thermophysical properties of real liquids can be estimated using hard-sphere models because the repulsive part of the intermolecular potential dominates the properties at high densities [9]. The smooth-hard-sphere (SHS) theory [12] can be applied to correlate the dimensionless viscosity, thermal conductivity and self-diffusion coefficients of pure fluids obtained from molecular simulations as functions of reduced volume V^*. Here, V^* is defined as V/V_0, where V is molar volume and V_0 is the molar core volume which, for hard-sphere of diameter σ, is $N_A \sigma^3 / \sqrt{2}$, where N_A is Avagadro's constant. As an example, the dimensionless self-diffusion coefficient D_{11}^* is defined by

$$D_{11}^* = \frac{[nD_{11}]}{[nD_{11}]_0} \left(\frac{V}{V_0}\right)^{2/3} = \left(2N_A\right)^{1/3} \frac{8\sqrt{\pi}}{3} \left(\frac{M}{RT}\right)^{1/2} \left(\frac{D_{11}}{V^{1/3}}\right), \qquad (2)$$

where D_{11} is the self-diffusion coefficient, n is number density, and $[nD_{11}]_0 = (3/8\sigma^2)(RT/\pi M)^{1/2}$ is the kinetic-theory expression for the dilute-gas limit of nD_{11}. This dimensionless self-diffusion coefficient is correlated as a function of V^* only:

$$D_{11}^* = F_{11}(V^*), \qquad (3)$$

where $F_{11}(V^*)$ is a universal function [13, 14]. The same theory can be applied to real spherical molecules when V_0 is treated as a weakly temperature-dependent parameter. It is found that both molecular simulation data for smooth hard-spheres and experimental data for real monatomic gases conform to this model.

Non-spherical molecules have internal energy that may be exchanged in collisions and such systems are treated as rough hard-spheres (RHS) [15]. In the RHS theory, an additional temperature- and density-independent 'roughness factor' appears such that, for example, the dimensionless self-diffusion coefficient is defined by

$$D_{11}^* = \left(2N_A\right)^{1/3} \frac{8\sqrt{\pi}}{3A_{11}} \left(\frac{M}{RT}\right)^{1/2} \left(\frac{D_{11}}{V^{1/3}}\right), \qquad (4)$$

where A_{11} is the roughness factor and $0 \leq A_{11} \leq 1$. The universal function F_{11} remains the same and experimental data for a given substance are correlated by determining the optimal values of A_{11} and of a small set of parameters that describe V_0 as a function of T.

The tracer diffusion coefficients D_{12} for RHS systems can be treated theoretically in a similar way [12]. The method has been further developed and applied to real systems by Cadogan et al. [10] in terms of a dimensionless tracer diffusion coefficient D_{12}^* for solute 1 in solvent 2 defined as follows:

$$D_{12}^* = \left(2N_A\right)^{1/3} \frac{8\sqrt{\pi}}{3A_{12}} \left(\frac{2M_{12}}{RT}\right)^{1/2} \left(\frac{V_{0,12}}{V_{0,2}}\right)^{2/3} \left(\frac{D_{12}}{V^{1/3}}\right). \tag{5}$$

here, A_{12} is the corresponding roughness factor, $M_{12} = M_1 M_2 / (M_1 + M_2)$ is the reduced molar mass, $V_{0,2}$ is the molar core volume of the solvent, $V_{0,12} = (V_{0,1}^{1/3} + V_{0,2}^{1/3})^3 / 8$, and $V_{0,1}$ is the molar core volume of the solute.

For hard spherical molecules, D_{12}^* is rigorously a function of the reduced volume V^* and of the two ratios $V_{0,2} / V_{0,1}$ and M_2 / M_1 where $V_{0,i} = N_a \sigma_i^3 / \sqrt{2}$ and σ_i is the diameter of molecule of type i. However, analysis of the tracer diffusion coefficient data for smooth hard-sphere mixtures, obtained by molecular dynamics simulations [16], showed that D_{12}^* can be represented by a function of just two variables: the reduced volume $V^* = V / V_{0,2}$ and the 'asymmetry' ratio χ defined by [10]

$$\chi = M_1 V_{0,2} / (M_2 V_{0,1}). \tag{6}$$

Therefore, in general, we have

$$D_{12}^* = F_{12}(V^*, \chi), \tag{7}$$

where $F_{12}(V^*, \chi)$ is a universal function to be determined. An attractive feature of Eqs. 5 and 7 is that they treat tracer diffusion in binary systems in a similar way to the RHS theory for the transport properties of pure substances. In particular, the approach reduces to the established RHS correlation for the self-diffusion coefficient when the solute and solvent become identical.

The molar core volumes $V_{0,i}(T)$ in Eq. 5 are expected to be identical with those determined from the pure-component properties. As discussed in the literature, these are weak functions of temperature and may be obtained by analysis of the transport properties of each pure substance in the high-density region where the rough hard-sphere theory is valid. Proceeding on this basis, Cadogan et al. [10] analysed their experimental mutual diffusion coefficient data for dilute solutions of CO_2 in various hydrocarbon liquids. These systems were characterised by a nearly constant asymmetry ratio $\chi = 2.1$ and, for that class of mixtures, the data were represented by means of a simple polynomial:

$$F_{12}(V^*, \chi = 2.1) = \sum_{i=0}^{3} a_i (V*)^i. \tag{8}$$

The model therefore required just one system-dependent parameter, A_{12}, and four universal constants a_i, in addition to the molar core volumes of the pure components. The purpose of the present work is to extend this methodology to encompass a wider range of non-polar solutions and to obtain the dependence of F_{12} on both V^* and χ.

The RHS theory for tracer diffusion in binary systems has also been studied by Akgerman and co-workers in a series of papers published between 1987 and 1997 [17–20]. The models derived in that work corresponds to an assumption that F_{12} is a linear function of V^* and that the dependence upon χ can be absorbed into a prefactor. The final form of their model is very simple:

$$D_{12}\Big/\sqrt{T} = \beta(V - V_D), \tag{9}$$

where V_D is a close-packed molar volume (generally different to V_0) at which diffusion effectively ceases and β is a scaling parameter. In an attempt to make the model predictive, β and V_D have been correlated in various forms. For example, Eaton et al. [20] correlated β and V_D with the critical constants of the solute and solvent in terms of universal constants which were adjusted by comparison with experimental data for the diffusion coefficient of 1-octene in supercritical alkane solvents. When compared with more than 1500 data points from the literature for other binary systems, the average absolute relative deviation (Δ_{AARD}) was found to be approximately 15 %. However, it turns out that experimental data (e.g. for CO_2 in squalane) do not conform to the linear dependence upon V embodied in Eq. 9. Therefore, we prefer the more general representation offered by Eq. 7.

3 Basis of the New Correlation

To extend the RHS model, we considered experimental data for the tracer diffusion coefficients of a range of gaseous solutes in hydrocarbon solvents, together with molecular dynamics simulations for systems of smooth hard-spheres. The simulation data anchor the correlation because, for these SHS systems, $A_{12} = 1$ by definition.

3.1 Experimental Data

Table 1 summarises the data retrieved from the literature for the solute–solvent systems that were used in this study, including the temperature and pressure ranges, the number of data points, the measurement techniques and the estimated uncertainty of the measurements. Most of the systems were studied using the Taylor dispersion method which is generally a reliable technique with relative uncertainties of between 1 and 3 %. Higher uncertainties were found for systems studied using capillary cells and Mach–Zehnder interferometers. The most well studied systems are solutions of CH_4 and CO_2 in hydrocarbon liquids, with data extending over substantial ranges of temperature and pressure. The other systems present data mainly at atmospheric pressure.

Table 1 Summary of experimental diffusion coefficients data from the literature, where T is temperature, p is pressure, N is number of data points and U_r is expanded relative uncertainty ($k=2$)

Solute	Solvent	T/K	p/MPa	N	Method	$10^2\ U_r$	Ref.
CH_4	Hexane	298	0.3	1	TD	<3	[21]
	Heptane	323–398	1–63	19	TD	2.3	[11]
	Octane	298–403	0.1	3	TD	1	[22]
		281–312	1.7	4	CAR	0.2	[23]
		304–435	1.72	6	TD	1	[24]
	Nonane	281–312	1.7	4	CAR	0.2	[23]
	Decane	298	0.3	1	TD	1.4	[21]
		298–433	0.1	3	TD	1	[22]
		281–312	1.7	4	CAR	0.2	[23]
	Dodecane	298	0.1	1	CC	3	[25]
	Methylbenzene	323–398	1–65	20	TD	2.3	[11]
C_2H_6	Hexane	298	0.1	1	CC	14	[26]
		303	0.1	1	CC	3	[27]
	Heptane	303–313	0.1	2	CC	3	[27]
		298	0.1	1	CC	14	[26]
	Octane	304–435	1.72	6	TD	1	[24]
		298	0.1	1	CC	14	[26]
	Dodecane	298	0.1	1	CC	14	[26]
C_3H_8	Hexane	298	0.1	1	CC	<5	[28]
	Heptane	298	0.1	1	CC	<5	[28]
	Octane	298	0.1	1	CC	<5	[28]
		335–435	1.72	6	TD	1	[24]
CO_2	Hexane	298–423	1.2–66	16	TD	2.6	[10]
	Heptane	298–423	1–68	30	TD	2.6	[10]
	Octane	298–423	0.9–69	30	TD	2.6	[10]
	Decane	298–423	1.1–68	16	TD	2.6	[10]
	Dodecane	298–423	1.3–63	15	TD	2.6	[10]
	Hexadecane	298–423	1–69	27	TD	2.6	[10]
	Squalane	298–423	1–67	30	TD	2.6	[10]
	Methylbenzene	298–423	1–68	30	TD	2.6	[10]
Ar	Hexane	298	0.3	1	TD	<3	[21]
	Octane	298–373	0.1	3	TD	1	[22]
	Decane	298–333	0.1	2	TD	1	[22]
N_2	Octane	303–399	15	4	MZI	10	[29]
	Decane	298–422	7.5–15	11	MZI	10	[29]

TD Taylor dispersion, *CAR* cylindrical acoustic resonance, *MZI* Mach–Zehnder interferometer, *CC* capillary cell

In order to analyse the experimental data, we required correlations for the molar core volumes as functions of temperature. These were mostly obtained from the literature and, for ease of reference, the relevant equations are reproduced in Table 2. New

Table 2 Correlations for the molar core volume for different compounds as functions of temperature, where $\theta = T/K$ and $C =$ carbon number

Compound	Correlation for $V_0/(\text{cm}^3\ \text{mol}^{-1})$	Ref.
(C$_1$ to C$_4$) alkanes	$45.822 - 6.1867\,\theta^{1/2} + 0.368\,79\,\theta - 0.007\,273\,\theta^{3/2} + C\,(2.178\,71\,\theta^{1/2} - 0.185\,198\,\theta + 0.004\,00369\,\theta^{3/2}) + C^2\,(6.951\,48 - 52.6436\,\theta^{-1/2}) + C_n^3\,(-7.801\,897 + 42.244\,93\,\theta^{-1/2} + 0.447\,6523\,\theta^{1/2} - 0.009\,573\,512\,\theta)$	[30, 31]
(C$_6$ to C$_{12}$) alkanes	$117.874 + 0.15\,(-1)^C - 0.252\,75\,\theta + 0.000\,548\,\theta^2 - 4.246 \times 10^{-7}\,\theta^3 + (C - 6)\,(1.27 - 0.0009\,\theta)\,(13.27 + 0.025\,C)$	[30, 31]
Hexadecane	$276.144 - 0.2384\,\theta + 0.000\,169\,83\,\theta^2$	[32]
Squalene	$631.293 - 0.9545\,\theta + 0.000\,903\,51\,\theta^2$	[33, 34]
Methylbenzene	$92.929 - 0.109\,30\,\theta + 0.000\,120\,23\,\theta^2$	[35]*
CO$_2$	$25.802 - 0.025\,251\,\theta + 0.000\,017\,948\,\theta^2$	[33, 34]
Argon	$7.823 + 12.520 \cdot \exp(-\theta/325.78)$	This work
Nitrogen	$12.545 + 13.298 \cdot \exp(-\theta/171.27)$	This work

*Eq. 12 in reference [35] is missing a term $+ 12.163C$ [Assael, personal communication]

correlations for $V_0(T)$ were developed for nitrogen and argon in a form that presents reasonable extrapolation behaviour at high temperatures. For these components, it was found that the available viscosity data could be represented by the extended hard-sphere mode of Ciotta et al. using a simple-three-parameter model for $V_0(T)$ as follows:

$$V_0 = a - b\exp(-T/c), \tag{10}$$

The development of these V_0 correlations is detailed in the Supplementary Information.

3.2 Molecular Simulation Data

Table 3 summarises the available molecular dynamics (MD) data for self- and mutual-diffusion coefficients in hard-sphere systems. Only three studies report data for mutual diffusion coefficients of binary SHS systems and, among these, the results of Easteal and Woolf [36] are the most comprehensive and accurate. The MD data are reported in the form of the ratio

$$C_{12} = \frac{[nD_{12}]}{[nD_{12}]_E}, \tag{11}$$

where n is number density, $[nD_{12}]_E$ is given by Enskog's expression,

$$[nD_{12}]_E = \frac{[nD_{12}]_0}{g_{12}(\sigma_{12})}, \tag{12}$$

Table 3 Molecular dynamics simulation data for the self- and mutual-diffusion coefficients of smooth hard-sphere systems, where σ_i is the diameter and m_i the mass for molecules of type i, V is the molar volume, $V_{0,i} = N_a \sigma_i^3 / \sqrt{2}$, N is the number of data points and U_r is the expanded relative uncertainty ($k=2$)

Authors	$V/V_{0,2}$	σ_2/σ_1	m_2/m_1	N	$10^2\, U_r$	Ref.
Easteal and Woolf (1990)	1.5–2	1–2	0.6–10	360	2–3	[16]
Alder et al. (1974)	1.5–3	1–4	1–5625	48	Not specified	[38]
Herman and Alder (1972)	1.6–3	1	0.25–5625	10	Not specified	[39]
Woodcock (1981)	1.3–1.5	1	1	15	Not specified	[40]
Easteal et al. (1983 &1984)	1.5–4	1	1	54	2–3	[36, 41]
Alder et al. (1970)	1.5–100	1	1	24	Not specified	[42]
Erpenbeck et al. (1991)	1.6–25	1	1	10	Not specified	[43]

$[nD_{12}]_0 = (3/8\sigma_{12}^2)(RT/2\pi M_{12})^{1/2}$ is the value of nD_{12} in the dilute-gas limit, $\sigma_{12} = \frac{1}{2}(\sigma_1 + \sigma_2)$, and $g_{12}(\sigma_{12})$ is the value of the unlike radial distribution function at contact. Hence, in terms of C_{12} the dimensionless tracer diffusion coefficient is given by

$$D_{12}^* = \frac{C_{12}}{g_{12}(\sigma_{12})}\left(\frac{V}{V_0}\right)^{2/3}. \tag{13}$$

In order to recover D_{12}^* we obtained $g_{12}(\sigma_{12})$ from the relation

$$g_{12}(\sigma_{12}) = \frac{1}{1-\xi} + \frac{3\xi}{(1+\sigma_2/\sigma_1)(1-\xi)^2} + \frac{\xi^2}{(2\sigma_2/\sigma_1)(1-\xi)^3}, \tag{14}$$

where $\xi = \pi n \sigma_2^3/6 = \pi\sqrt{2}/(6V^*)$ is the solvent packing density [37, 38].

4 Results and Discussion

For the chosen combinations of solutes and solvents, the asymmetry ratio χ covers a range from approximately 0.8 to 3.1. These ratios are only weak functions of temperature and this is illustrated in Fig. 1 for five solutes (CH_4, C_3H_8, N_2, CO_2 and Ar) in octane.

For a given solute, the values of χ in different alkane solvents are very similar, although the corresponding values in the aromatic solvent methylbenzene are about 15 % smaller. For the hard-sphere systems, the data set of Easteal and Woolf was limited to combinations of $\sigma_1/\sigma_2 \leq 1$ and $M_1/M_2 \leq 1$, representative of 'light' solutes in 'heavy' solvents. Figure 2 shows the simulation data for SHS as a function of χ for three different values of reduced volume. From this we deduced that the dependence upon χ is approximately linear. Therefore, the trial function for $F_{12}(V^*, \chi)$ was a simple extension of Eq. 8:
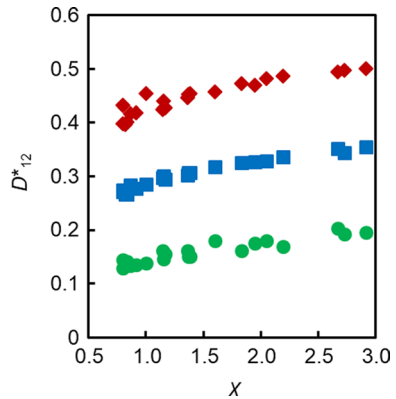
$$F_{12}(V^*, \chi) = \sum_{i=0}^{3} a_i (V^*)^i + b_0 \chi. \tag{15}$$

**Fig. 1** Asymmetry ratios χ for five solutes in octane as functions of temperature T
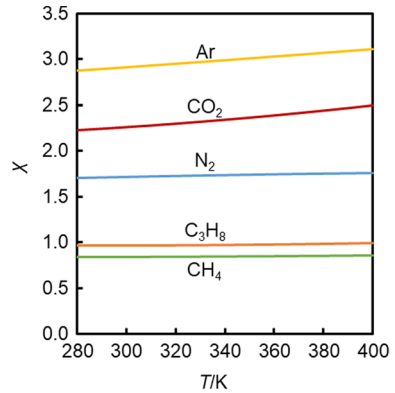
Fig. 2 Dimensionless tracer diffusion coefficients of SHS systems as a function of the asymmetry ratio χ for various reduced volumes: ● $V* = 1.5$; ■ $V* = 1.7$; ◆ $V* = 1.9$ [16]

For hard-spheres, $A_{12} = 1$ by definition while, for real fluids, A_{12} is a constant for each solute–solvent pair. The parameters a_i ($i = 0, 3$) and b_0 together with the roughness factor for each real-fluid solute–solvent pair were then adjusted in a non-linear optimisation. The objective function to be minimised was the un-weighted sum of the squares of the relative deviations of the data from the model. Because of the limited range of validity of the correlations for $V_0(T)$, the data in n-alkane solvents up to dodecane were limited to a maximum temperature of 411 K.

This simple model proved to provide a good account of the data as illustrated in Figs. 3 and 4 with deviations mostly within ± 5 %. Figure 3 compares the data for different solutes with the model as functions of the reduced volume $V*$ of the solvent, where the model curve is plotted for the mean value of χ applicable to each solute gas. Figure 4 shows the relative deviations of the data from the model as functions of T, $V*$, M_1/M_2 and χ. The comparison shows mostly good agreement but some evidence of systematic deviations for larger values of $V*$. However, generally, the deviation plots do not suggest that additional parameters in the universal function would improve the overall representation. In Fig. 3, the SHS data are for self-diffusion ($\chi = 1$), while all of the SHS data considered are included in Fig. 4.

Table 4 reports the values of the universal coefficients determined in the fit, while Table 5 lists the roughness factors obtained and the values of the average absolute
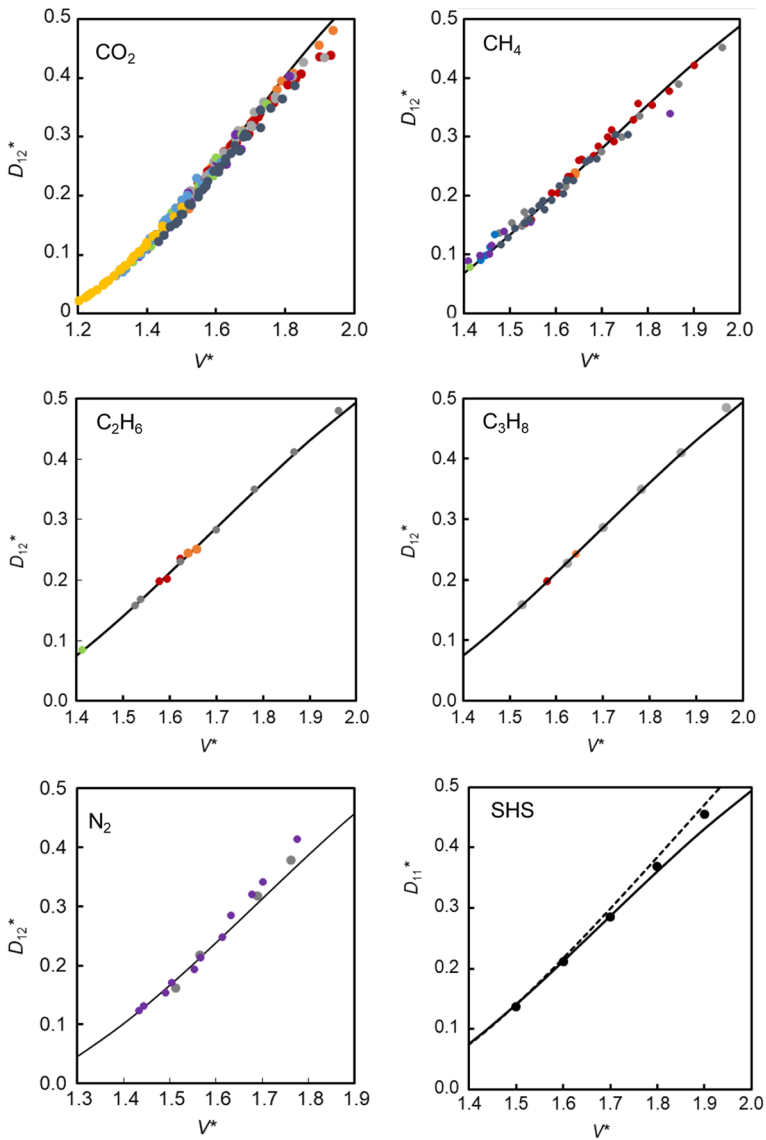
Fig. 3 Dimensionless tracer diffusion coefficients D_{12}^* or self-diffusion coefficients D_{11}^* as function of the reduced volume V^* of the solvent for different solutes. Experimental data for different solvents: ⬤ hexane; ⬤ heptane; ⬤ octane; ⬤ nonane; ⬤ decane; ⬤ dodecane; ⬤ hexadecane; ⬤ squalane; ⬤ methylbenzene. ⬤ Molecular simulation data for the self-diffusion coefficients of smooth hard-spheres (SHS). ——— RHS theory plotted for a representative value of χ for each solvent system; - - - - - - correlation for the dimensionless self-diffusion coefficient of SHS [13]

relative deviation (Δ_{AARD}) and the maximum absolute relative deviation (Δ_{MARD}). Entries without values of Δ_{AARD} and Δ_{MARD} are for systems with only a single data point available from which A_{12} was determined.
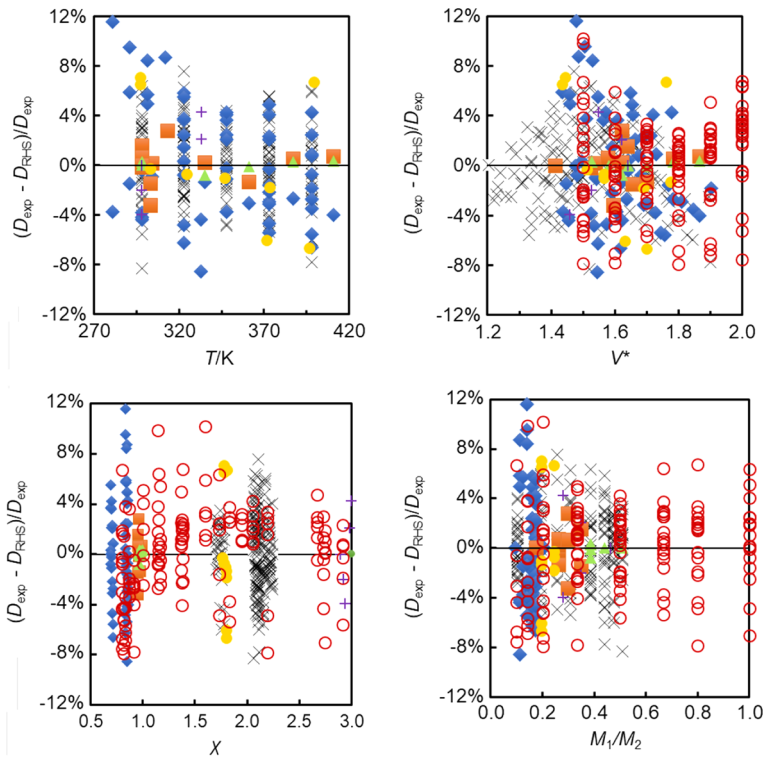
Fig. 4 Relative deviations $(D_{exp} - D_{RHS})/D_{exp}$ of experimental or simulated tracer diffusion coefficients from the RHS model as function of temperature T, reduced volume $V/V_{0,2}$, molar mass ratio M_1/M_2 and asymmetry ratio χ, where 1 denotes solute and 2 denotes solvent. Symbols indicate solutes: ×CO_2; ◆ CH_4; ■ C_2H_6; ▲ C_3H_8; ● N_2; + Ar; ○ smooth hard-sphere

Table 4 Values of the parameters a_i and b_0 in the universal curve for tracer diffusion coefficients, together with the average absolute relative deviation (Δ_{AARD}) and the maximum absolute relative deviation (Δ_{MARD}) for the fit

Parameter	Value
a_0	1.6874
b_0	0.0341
a_1	−4.0605
a_2	2.8478
a_3	−0.5621
Δ_{AARD}	2.7 %
Δ_{MARD}	11.6 %

Application of the model to a new compound requires at least one experimental value of the tracer diffusion coefficient and sufficient pure-component data to determine $V_0(T)$. The model is only correlative because we presently have no means of predicting the roughness factors. Figure 5 shows some of the roughness factors determined for different solutes in alkane solvents. For CO_2 as the solute, there is a clear

Table 5 Roughness factors A_{12} for different systems with absolute average relative deviations Δ_{AAD} and maximum absolute relative deviations Δ_{MAD} for the diffusion coefficient

Solute	Solvent	A_{12}	Δ_{AAD} (%)	Δ_{MAD} (%)
CH_4	Hexane	0.771	0.4	0.4
	Heptane	0.647	3.2	6.2
	Octane	0.765	5.0	11.6
	Nonane	0.898	0.2	5.7
	Decane	0.779	0.0	0.0
	Dodecane	0.731	6.1	8.7
	Benzene	1.079		
	Methylbenzene	0.858	2.8	6.6
C_2H_6	Hexane	0.732	1.5	1.5
	Heptane	0.800	2.2	3.2
	Octane	0.792	0.5	1.4
	Dodecane	0.749		
C_3H_8	Hexane	0.788		
	Heptane	0.827		
	Octane	0.845	0.4	0.8
CO_2	Hexane	0.942	2.2	8.3
	Heptane	0.915	3.1	7.8
	Octane	0.871	2.3	6.4
	Decane	0.788	4.0	6.3
	Dodecane	0.750	2.6	7.6
	Hexadecane	0.706	3.3	6.0
	Squalane	0.514	1.5	4.0
	Methylbenzene	1.161	1.9	6.0
Ar	Hexane	0.763		
	Octane	0.760	2.0	2.1
	Decane	0.653	4.1	4.3
N_2	Octane	0.761	4.4	8.2
	Decane	0.761	3.8	7.1
SHS	SHS	1.000	2.9	10.2

trend with carbon number but the same cannot be said for CH_4 or C_2H_6. It is possible that new experimental data might result in smoother trends but, for now, the evidence is that A_{12} does not depend systematically upon the carbon number of the solvent for alkane-alkane systems. On the other hand, the smooth trend for CO_2-alkane systems suggest that the diffusion coefficients for CO_2 in other alkanes could be predicted.

Although the model has been developed for hydrocarbon solvents with inorganic and light hydrocarbon solutes, the method might be expected to apply to other non-polar solute–solvent systems. As presented, the correlation is restricted to light solutes. Preliminary investigation suggests that a more complex form of the universal function would be required to encompass also 'heavy' solutes in 'light' solvent and this might be developed using available experimental data for large molecular solutes in light supercritical solutes and also the molecular simulation data that were excluded from the present analysis (those with $\sigma_1/\sigma_2 > 1$ and/or $M_1/M_2 > 1$).

Fig. 5 Roughness factors A_{12} for various solutes in alkane solvents of carbon number C_n: ● CO_2; ■ CH_4; ◆ C_2H_8
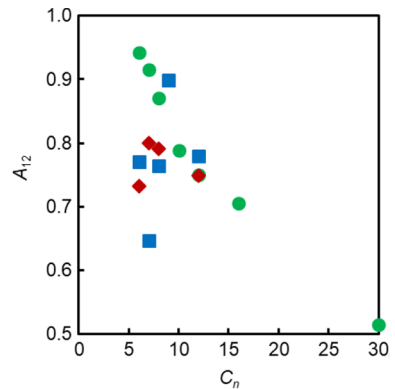
5 Conclusions

The model presented in this paper allows tracer diffusion coefficients to be rationalised within the well-established hard-sphere theory used to correlate and predict the transport properties of pure substances. To model a particular system one requires the molar core volume of both the solute and the solvent, as determined from pure-component transport properties, and the value of the roughness factor A_{12} specific to the solute–solvent pair. Once A_{12} is known, the model may be used to predict tracer diffusion coefficient over wide ranges of temperature and density. The method has been tested for non-polar systems comprising a light solute in a heavier solvent at reduced densities $1/V^* \geq 0.5$. For CO_2 in alkane solvents, the roughness factor shows a clear systematic dependence upon the carbon number of the solvent but generally no clear relationship between A_{12} and the nature of the solute and solvent emerges. We note that the available experimental data against which to test the model is quite restricted and that new measurements over extended ranges of temperature and pressure would be helpful. Future work might also focus on extending the model to wider ranges of size and mass ratios.

References

1. C. Zhang, C. Qiao, S. Li, Z. Li, Energies **11**, 1495 (2018)
2. M. Ghoroori, A. Shahrabadi, M. Jamialahmadi, Energy Sources A **39**, 36 (2017)
3. P. Behnoudfar, A. Rostami, A. Hemmati-Sarapardeh, in *Fundamentals of enhanced oil and gas recovery from conventional and unconventional reservoirs*. ed. by A. Bahadori (Gulf Professional Publishing, Houston, 2018), pp. 101–138
4. D. Janiga, R. Czarnota, E. Kuk, J. Stopa, P. Wojnarowski, J. Pet. Sci. Eng. **185**, 106636 (2020)
5. M. Jamialahmadi, M. Emadi, H. Müller-Steinhagen, J. Pet. Sci. Eng. **53**, 47 (2006)
6. C. Dariva, L.A.F. Coelho, J.V. Oliveira, Fluid Phase Equilib. **158**, 1045 (1999)
7. A.D. Michael, *The No-Slip Condition of Fluid Dynamics* (Kluwer Academic, Dordrecht, 1990)
8. D.M. Himmelblau, Chem. Rev. **64**, 527 (1964)
9. M.R. Riazi, C.H. Whitson, Ind. Eng. Chem. Res. **32**, 3081 (1993)
10. S.P. Cadogan, B. Mistry, Y. Wong, G.C. Maitland, J.P.M. Trusler, J. Chem. Eng. Data **61**, 3922 (2016)
11. M.B.M. Taib, J.P.M. Trusler, Int. J. Thermophys. **41**, 119 (2020)
12. C.M. Silva, H. Liu, in *Theory and simulation of hard-sphere fluids and related systems*. ed. by Á. Mulero (Springer, Berlin, 2008), pp. 383–492
13. J.H. Dymond, M.J. Assael, in *Transport properties of fluids : their correlation, prediction and estimation*. ed. by J. Millat, J.H. Dymond, C.A. Nieto de Castro (Cambridge University Press, Cambridge, 1996), pp. 226–249
14. M.J. Assael, J.H. Dymond, V. Tselekidou, Int. J. Thermophys. **11**, 863 (1990)
15. D. Chandler, J. Chem. Phys. **62**, 1358 (1975)
16. A.J. Easteal, L.A. Woolf, Chem. Phys. Lett. **167**, 329 (1990)
17. M.A. Matthews, A. Akgerman, J. Chem. Phys. **87**, 2285 (1987)
18. C. Erkey, A. Akgerman, AlChE J. **35**, 1907 (1989)
19. C. Erkey, J.B. Rodden, M.A. Matthews, A. Akgerman, Int. J. Thermophys. **10**, 953 (1989)
20. A.P. Eaton, A. Akgerman, Ind. Eng. Chem. Res. **36**, 923 (1997)
21. D.F. Evans, T. Tominaga, H.T. Davis, J. Chem. Phys. **74**, 1298 (1981)
22. S.H. Chen, H.T. Davis, D.F. Evans, J. Chem. Phys. **77**, 2540 (1982)
23. S.O. Colgate, V.E. House, V. Thieu, K. Zachery, J. Hornick, J. Shalosky, Int. J. Thermophys. **16**, 655 (1995)
24. C. Erkey, A. Akgerman, AlChE J. **35**, 443 (1989)
25. W. Hayduk, W.D. Buckley, Chem. Eng. Sci. **27**, 1997 (1972)
26. W. Hayduk, S.C. Cheng, Chem. Eng. Sci. **26**, 635 (1971)
27. V.K. Malik, W. Hayduk, Can. J. Chem. Eng. **46**, 462 (1968)
28. W. Hayduk, R. Castaneda, H. Bromfield, R.R. Perras, AlChE J. **19**, 859 (1973)
29. S. Killie, B. Hafskjold, O. Borgen, S.K. Ratkje, E. Hovde, AlChE J. **37**, 142 (1991)
30. M.J. Assael, J.H. Dymond, M. Papadaki, P.M. Patterson, Int. J. Thermophys. **13**, 269 (1992)
31. M.J. Assael, J.P.M. Trusler, T.F. Tsolakis, *Thermophysical Properties of Fluids: An Introduction to Their Prediction* (Imperial College Press, London, 1996)
32. F. Ciotta, J.P.M. Trusler, V. Vesovic, Fluid Phase Equilib. **363**, 239 (2014)
33. F. Ciotta, G. Maitland, M. Smietana, J.P.M. Trusler, V. Vesovic, J. Chem. Eng. Data **54**, 2436 (2009)
34. F. Ciotta, G. Maitland, M. Smietana, J.P.M. Trusler, V. Vesovic, J. Chem. Eng. Data **55**, 4126 (2010)
35. M.J. Assael, J.H. Dymond, P.M. Patterson, Int. J. Thermophys. **13**, 895 (1992)
36. A.J. Easteal, L.A. Woolf, D.L. Jolly, Phys. A **121**, 286 (1983)
37. J.L. Lebowitz, Phys. Rev. A **133**, 895 (1964)
38. B.J. Alder, W.E. Alley, J.H. Dymond, J. Chem. Phys. **61**, 1415 (1974)
39. P.T. Herman, B.J. Alder, J. Chem. Phys. **56**, 987 (1972)
40. L.V. Woodcock, Ann. N. Y. Acad. Sci. **371**, 274 (1981)
41. A.J. Easteal, L.A. Woolf, D.L. Jolly, Phys. A **127**, 344 (1984)
42. B.J. Alder, D.M. Gass, T.E. Wainwright, J. Chem. Phys. **53**, 3813 (1970)
43. J.J. Erpenbeck, W.W. Wood, Phys. Rev. A **43**, 4254 (1991)